A Comparison of Palladium Sorption Using Polyethylenimine Impregnated Alginate-Based and Carrageenan-Based Algal Beads

Shengye Wang, Thierry Vincent, Catherine Faur, Eric Guibal

applied sciences

MDPI

Article

A Comparison of Palladium Sorption Using Polyethylenimine Impregnated Alginate-Based and Carrageenan-Based Algal Beads

Shengye Wang [1,*], Thierry Vincent [1], Catherine Faur [2] and Eric Guibal [1,*]

[1] C2MA, IMT Mines Ales, University of Montpellier, 30100 Ales, France; thierry.vincent@mines-ales.fr
[2] IEM, Institut Européen des Membranes, University of Montpellier, CNRS, ENSCM, 34090 Montpellier, France; Catherine.Faur@umontpellier.fr
* Correspondence: Shengye.Wang@mines-ales.fr (S.W.); Eric.Guibal@mines-ales.fr (E.G.); Tel.: +33-046-678-2734 (E.G.)

Received: 18 January 2018; Accepted: 6 February 2018; Published: 10 February 2018

Abstract: Two kinds of algal beads were prepared using a carrageenan-based alga (*Chrondrus crispus*) and an alginate-based alga (*Laminara digitata*) ionotropically gelled with K(I) and Ca(II), respectively: the process consists of biopolymer partial extraction followed by hydrogel formation. The beads were modified with branched polyethylenimine (bPEI) and glutaraldehyde (GA) using the impregnation method to improve their sorption capacity for Pd(II) in acid solution. SEM-EDX and FTIR techniques were used for characterizing the beads. The impacts of pH and presence of anions, cations, and Pt(IV) were studied in batch experiments. The beads were also applied for Pd(II) recovery from synthesized leaching liquors of a spent catalyst and a car catalytic converter via the sorption-desorption process. Results show that Pd is concentrated in the outer layer of *L. digitata*-bPEI-GA composite (LD/PEI) beads, while in the case of the *C. crispus*-bPEI-GA composite (CC/PEI), it is homogenously distributed in the whole mass of the sorbents. The difference is attributed to the repulsive force of the outer Ca(II)-alginate barrier of LD/PEI beads that makes it difficult for the branched polymer PEI to penetrate through the layer and be immobilized in the inner compartment. As a result, LD/PEI beads possess a lower maximum sorption capacity, but a slightly faster uptake at pH 1 than CC/PEI beads. In addition, CC/PEI beads present a better recovery performance compared to LD/PEI beads when applied for the treatment of synthesized leaching liquors.

Keywords: carrageenan; alginate; alga; polyethylenimine; palladium; recovery

1. Introduction

Palladium (Pd), one of the precious platinum group metals (PGMs), has been widely applied in electronic devices and automotive catalysts [1,2]. As one of the most extensively exploited precious metals, Pd is in short supply due to its rare source and increasing global demand [3]. However, waste electronic devices and catalysts are constantly produced due to the limitation of their lifetime [4]. Palladium, along with other PGMs, remains in the matrix of the supports. Therefore, efficient and economical methods for recovering such metal from its main waste streams, electronic devices, and catalysts, are highly needed for sustainably recycling Pd. The conventional methods for Pd recovery generally can be classified as pyrometallurgy and hydrometallurgy. The former category consists of separating Pd from the support by melting the crushed wastes at high temperatures and dissolving the metal in an acid matrix, while the later treatment, hydrometallurgy, refers to leaching the wastes using oxidant-acid solutions containing HNO_3, HCl, H_2O_2, or $AlCl_3$ [5]. These leachates are treated by conventional precipitation, solvent extraction, and/or adsorption for recovering Pd(II). Precipitation is not generally applicable (poorly selective), while solvent extraction can be used but is

suffering from a high cost; this method is specially tailored for large-scale recovery with a high target metal concentration (higher than 0.5 g L^{-1} [6,7]). For those leaching liquors containing low metal concentrations, base metals, and a relatively high acidity, the recovery process is rather challenging [8].

Sorption is a physiochemical process that involves the passive sorption and/or complexation of metals by sorbents and is well-known for its low operating cost, high efficiency in recovering metal ions from low-concentration effluents, and small-occupied space. Polyethylenimine (PEI), which has a unique branched/linear conformation, is a superior ligand to chelate PGMs. To make this material stable, several studies previously incorporated its crosslinked products into biopolymers, such as chitosan [9], carrageenan [10,11], and alginate [12,13]. However, very few studies were conducted on the direct use of the raw natural materials as supports for PEI. Very recently, glutaraldehyde (GA) crosslinked PEI (branched) was incorporated in brown algal biomass (*Laminara digitata*) beads through a green and convenient process, during which alginate is simultaneously extracted and used for immobilizing PEI-GA via calcium gelation. Theoretically, beads can also be prepared through this process using a kind of red algae, *Chrondrus crispus*, taking advantage of 60% carrageenan inside this material to gel with potassium. Moreover, the pKa of carboxyl groups on alginate and sulfate groups on *kappa*-carrageenan beads is approximately 4 and 2 [14], respectively, while that of tertiary amine groups on PEI was reported as 11.6 [15]. Therefore, when adjusting the PEI solution pH between 4 and 11, PEI can be loaded through electrostatic interaction between the positively charged amino groups and the negatively charged carboxyl groups on *L. digitata* (LD) beads or sulfate groups on *C. crispus* (CC) beads [16].

Based on the discussion above, this study aims to develop two algal-based sorbents modified with PEI by the impregnation method for recovering palladium from the leaching liquors. To improve their stability, the loaded PEI was crosslinked with GA as a post-treatment [17]. The beads were characterized using FTIR and SEM-EDX and compared for Pd(II) sorption by evaluating the impact of parameters such as solution pH, the presence of co-existing anions and metals, and by investigating the sorption isotherms and kinetics. At the end, the sorbents were applied for Pd(II) recovery from synthesized leaching liquors to assess their feasibility for practical applications.

2. Materials and Methods

2.1. Materials

The brown algae, *L. digitata*, and red algae, *C. crispus*, were supplied by SETALG (Pleubian, France). The biomasses were washed, dried, grinded, and sieved (<250 μm). Branched polyethyleneimine (bPEI, 50% (*w*/*w*) in water) and glutaraldehyde (GA, 50% (*w*/*w*) in water) were purchased from Sigma-Aldrich (Taufkirchen, Germany). Other reagents such as sodium carbonate, formic acid, and calcium chloride were supplied by Chem-Lab NV (Zedelgem, Belgium). Palladium(II) chloride was obtained from R.D. H (Seelze, Germany). The stock solution was prepared by dissolving 1 g of palladium(II) in 1 L of 1.1 M HCl solution.

2.2. Preparation of LD/PEI and CC/PEI Beads

Supplementary Materials Figure S1 shows the preparation process of the beads. CC beads were prepared by adding 10 g of *C. Crispus* (dry) to 200 mL of NaOH solution (1%, *w*/*w*), while LD beads were obtained by the contact of 10 g of *L. digitata* (dry) with 2 g of Na_2CO_3 (in 388 mL of Milli-Q water). These two suspensions were heated at 50 °C for 24 h. Thereafter, for CC beads, the mixture was cooled below 10 °C and dropped wisely into 1 L of a cold 0.3 M KCl solution (in an ice water bath); for LD beads, the suspension was distributed dropwise into a solution containing both $CaCl_2$ (1%, *w*/*w*) and formic acid, HCOOH (1%, *v*/*w*). The beads were kept in the solutions overnight and rinsed two times with deionized water (1 L for each time). A schematic representation of modifications of the beads using bPEI and GA is shown in Figure 1. Both types of beads were further modified using bPEI followed by reaction with a crosslinker (GA). Specifically, the beads were firstly maintained in

250 mL of bPEI solution (1%, *w*/*w*) with a pH of 7.5 and gently stirred for 3 h. Thereafter, the beads were rinsed twice and soaked in 1% (*w*/*w*) GA solution for 5 h. After this step, the hardened beads were thoroughly washed with deionized water and freeze-dried (−52 °C, 0.1 mbar, two days). The LD beads and CC beads impregnated with bPEI and GA solutions were marked as LD/PEI and CC/PEI beads, respectively.

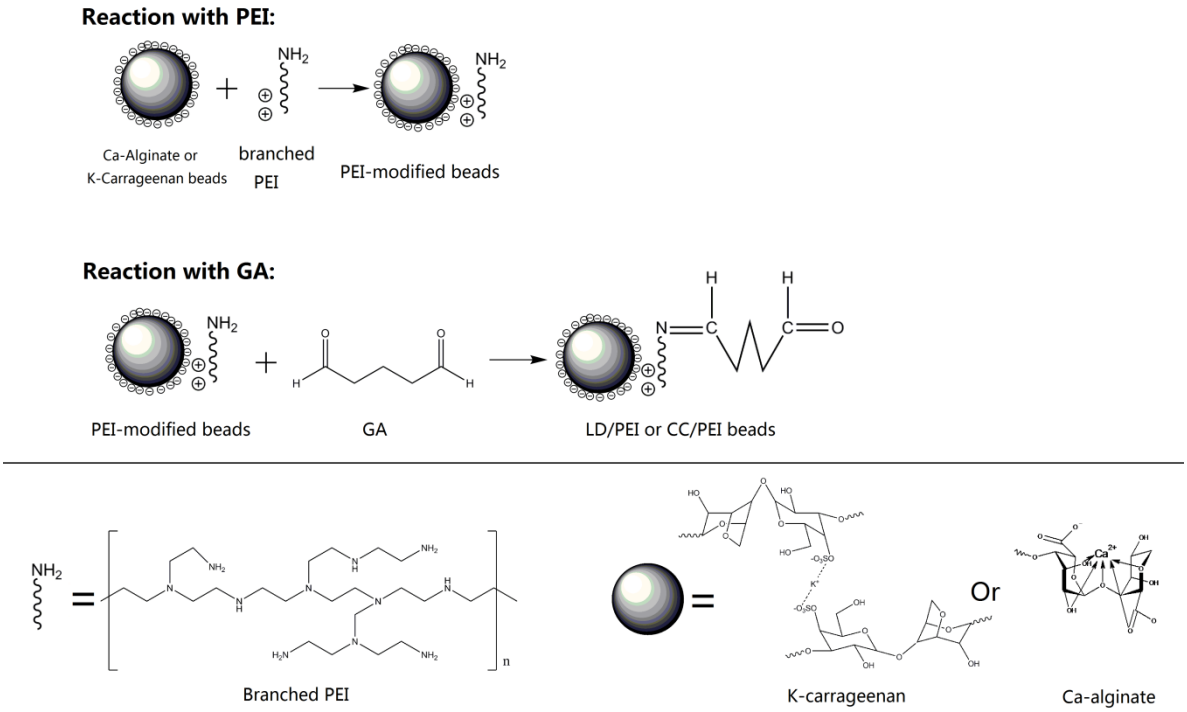

Figure 1. A schematic representation of modifications using bPEI and GA solutions. bPEI: branched polyethylenimine; GA: glutaraldehyde; LD/PEI: *L. digitata*-bPEI-GA composite; CC/PEI: *C. crispus*-bPEI-GA composite.

2.3. Characterization

Scanning electron microscopy (SEM) and SEM-EDX (SEM coupled with energy dispersive X-ray diffraction analysis) were performed using an environmental scanning electron microscope Quanta FEG 200 (FEI France, Thermo Fisher Scientific, Mérignac, France), equipped with an Oxford Inca 350 energy dispersive X-ray micro-analyzer (Oxford Instruments France, Saclay, France). FT-IR spectrometry analysis was performed in the range 4000–400 cm^{-1} using an FTIR-ATR (Attenuated Total Reflectance tool) Bruker VERTEX70 spectrometer (Bruker, Bremen, Germany). The Pd(II)-loaded beads for characterization of the metal-sorbent interaction were prepared by the contact of a Pd(II) solution (pH = 1; V = 20 mL; C_0 = 1.5 mmol Pd L^{-1}) with 10 mg of beads for 72 h.

2.4. Sorption in Mono-Metal System

The experiments to investigate the effect of pH were conducted within the initial pH range of 0.3–4 with a sorbent dosage of 0.25 g L^{-1} and contact time of 72 h at 20 °C. The pH of the solution was adjusted using H_2SO_4 or NaOH. The initial and final values of pH were measured using a pH-meter cyber scan pH 6000 (Eutech instruments, Nijkerk, The Netherlands). Sorption isotherms were carried out by the contact of the solutions containing different concentrations of Pd(II) with sorbents for 72 h at 20 °C. The sorbent dosage (SD) was 0.5 g L^{-1} (dry weight) and initial Pd(II) concentration (C_0, mmol Pd L^{-1}) varied between 0.05 and 2 mmol Pd L^{-1}. The residual metal concentration (C_{eq}, mmol Pd L^{-1}), after filtration, was analyzed by inductively coupled plasma atomic emission spectrometry (ICP-AES, JY Activa M, Jobin-Yvon, Horiba, Longjumeau, France).

The sorption capacity (q, mmol Pd g^{-1}) was calculated at equilibrium by the mass balance equation: $q_{eq} = (C_0 - C_{eq}) \cdot V/SD$. Uptake kinetics was studied with the sorbent dosage of 0.2 g L^{-1}, a Pd(II) concentration of 0.5 mmol L^{-1}, and initial solution pH of 1 adjusted by H_2SO_4. Samples were collected, filtrated, and analyzed for residual concentration using ICP-AES. The speciation of palladium under different conditions was calculated by Visual MINTEQ (version 3.0, 2011, KTH, Stockholm, Sweden).

2.5. Sorption in Complex System

The experiments for exploring the influence of anions or cations were carried out by contacting 20 mL of the solutions containing different concentrations of salts such as NaCl, Na_2SO_4, or $NaNO_3$ or $Fe_2(SO_4)_3$, $Al_2(SO_4)_3$, or $CuSO_4$ with a Pd(II) concentration of 0.75 ± 0.05 mmol L^{-1} with 5 mg sorbents for 72 h at 20 °C. The initial pH of the solution was adjusted to 1 using H_2SO_4 or NaOH. Palladium usually co-exists with other platinum group metals (such as platinum) in natural resources (ores, rocks, soils, and minerals) or in waste catalysts. The experiment for investigating the effect of Pt(IV) was conducted by contact of 20 mL of the solutions containing different concentrations of Pt(IV) with a fixed Pd(II) concentration of 0.5 mmol L^{-1} with 5 mg sorbents for 72 h at 20 °C. The initial pH of the solution was adjusted to 1 using H_2SO_4 or NaOH. To test the application potential of the beads for Pd(II) recovery, two kinds of leaching liquors were synthesized according to previous studies. One solution was simulated as the leaching liquor from spent catalyst containing 0.5 mmol L^{-1} of Pd(II), 2 M of NaCl, and 0.5 M of HCl [18,19], while the other one was an effluent coming from the dilution of a leaching solution of a car catalyst converter containing 0.4 mmol L^{-1} of Pd(II), 0.1 mmol L^{-1} of Pt(IV), 3.0 mmol L^{-1} of Fe(III), 91 mmol L^{-1} of Al(III), 2.5 mmol L^{-1} of Ce(III), 0.6 mmol L^{-1} of Zn(II), and 2 M H_2SO_4 [18,19]. The synthesized leaching liquors were treated by the sorption/desorption process. For the former liquor, a volume of 100 mL of the solution was treated with 100 mg of the beads for 72 h at 20 °C with a shaking speed of 150 rpm; for the latter one, the sorbent mass decreased to 50 mg while the other conditions remained the same. For the desorption process, 20 mL of 0.1 HCl/0.2 M thiourea solution was added to the well rinsed Pd-loaded beads, sealed, and placed in an oven at 50 °C for 24 h without shaking.

2.6. Modeling

Uptake kinetics have been modeled using the pseudo-first order rate equation (PFORE, Equation (1)) [20], the pseudo-second order rate equation (PSORE, Equation (2)) [21], and the resistance to the intraparticle diffusion equation (IPDE, Equation (3)) [22].

$$q_t = q_{eq}\left(1 - e^{-k_1 t}\right) \quad (1)$$

$$q_t = \frac{q_{eq}^2 k_2 t}{1 + q_{eq} k_2 t} \quad (2)$$

$$q_t = k_{id}\sqrt{t} + C \quad (3)$$

where q_t and q_{eq} (mmol g^{-1}) are the sorption capacities sorbed at t and at equilibrium, respectively. The parameters k_1, k_2, and k_{id} are the apparent rate constants of PFORE (h^{-1}), PSORE (g $mmol^{-1}$ h^{-1}), and IPDE (mmol g^{-1} $h^{-1/2}$), respectively. C is a constant of IPDE associated with the thickness of the boundary layer; a higher C value indicates a greater effect of the resistance to film diffusion (larger boundary layer). The parameters were also obtained by non-linear regression analysis using Origin 9.0 (Origin software Inc., San Clemente, CA, USA).

Sorption isotherms describe the distribution of metal ions between the liquid and the solid phases (when varying the metal concentration in the system). They plot the sorption capacity (i.e., q_{eq}) vs.

residual metal concentration (i.e., C_{eq}). Langmuir (Equation (4)) [23], Freundlich (Equation (5)) [24], and Sips (Equation (6)) [25] equations were used to fit the experimental data.

$$q_{eq} = \frac{q_{mL} b C_{eq}}{1 + b C_{eq}} \quad (4)$$

$$q_{eq} = K_F C_{eq}^{n} \quad (5)$$

$$q_{eq} = \frac{q_{mS} K_s C_{eq}^{1/n}}{1 + K_s C_{eq}^{1/n}} \quad (6)$$

where b (L $mmol^{-1}$) is the affinity coefficient and q_{mL} (mmol g^{-1}) is the sorption capacity at saturation of the monolayer in the Langmuir equation; K_F [(mmol g^{-1})/(mmol L^{-1})^n] is the Freundlich constant and n is the intensity parameter; $1/n$ is the heterogeneity factor, q_{mL} (mmol g^{-1}) is the maximum sorption capacity in the Sips equation, and K_s (L $mmol^{-1}$) is the affinity coefficient in the Sips equation. q_{eq} (mmol g^{-1}) is the amount of palladium uptake at equilibrium and C_{eq} (mmol L^{-1}) is the palladium concentration at equilibrium. The parameters were also obtained by non-linear regression analysis using Origin 9.0. The objectives of the modeling of sorption isotherms may consist of:

(a) the determination of the sorption capacities in function of the residual metal concentration (principle of the sorption isotherms); this may be helpful for predicting the sorption capacity under selected experimental conditions, where a good fit is of great importance;
(b) an approach of binding mechanism (the hypotheses attached to the model are indicative of mechanisms possibly involved in metal binding; however, the mathematical fit does not necessarily mean that the hypothesized mechanisms are fulfilled; this should be confirmed by physico-chemical analyses);
(c) the determination of maximum sorption capacities (saturation level) and the affinity (correlated to the initial slope of the curve) between the sorbent and the solute under selected experimental conditions (for the comparison of sorbents).

2.7. Statistical Analysis

Selected experiments were duplicated. Average values and standard deviations were calculated. In addition, the sorption capacities of the beads prepared at two different times were compared (shown in Supplementary Materials Figure S2) to evaluate the reproducibility of their synthesis. Data were tested for statistical significance with one way analysis of variance (ANOVA). The value of $p = 0.045$ ($p < 0.05$) indicates that the synthesis of the sorbents is reproducible.

3. Results and Discussion

3.1. Characterization

The SEM micrographs shown in Figure 2 clearly illustrate the porous structure of the beads. LD/PEI beads are characterized as more opened scaffolds with larger holes in the core of the beads compared to CC/PEI: the drying of the beads caused a more irregular surface for LD/PEI materials. The results of EDX analysis of the sorbents before and after Pd(II) sorption are shown in Supplementary Materials Figure S3. O and Ca elements in LD/PEI, and S and K in CC/PEI beads are associated with the embedding matrices. S in LD/PEI could be associated with fucoidan residues in the brown algae, while Na is due to the extraction process of the polymers (alginate or carrageenan), using Na_2CO_3 and NaOH, respectively. EDX spectra of the beads after metal sorption suggest that Pd(II) has been successfully loaded. Moreover, Ca in LD/PEI beads is not detectable. However, no Ca-Pd ion exchange should occur since chloro-palladium complex anions are predominant (discussed in Section 3.2). Hence, the disappearance of the Ca peak is probably due to the Ca(II)-Na(I) or Ca(II)-H(I) exchange reaction (the pH of the initial solution (pH < 1) was adjusted to 1 using NaOH solution).

Similarly, for CC/PEI beads after Pd(II) sorption, K is replaced by Na. The element cartographies of the cross-sections of the beads after Pd(II) sorption (shown in Figure 2) show that Pd is concentrated in the outer layer of LD/PEI beads, while for CC/PEI, it is homogeneously distributed in the whole mass of the beads. This phenomenon is probably due to the repulsive force of the outer Ca(II)-alginate barrier ("egg box" junctions) of LD/PEI beads; it is difficult for the branched polymer PEI to penetrate through the layer and get access to the internal compartment, resulting in a lower amount of loaded PEI inside LD/PEI. As a result, the metal uptake of LD/PEI beads is expected to be lower than that of CC/PEI (see next section). The distribution of Cl element is consistent with Pd distribution, confirming that Pd(II) is sorbed under the form of chloro-palladium complexes. The specific surface areas of dried beads (prepared by relatively similar procedures) were previously determined and showed values that did not exceed a few $m^2\ g^{-1}$, two orders of magnitude lower than the values reached with activated carbon or some synthetic resins.

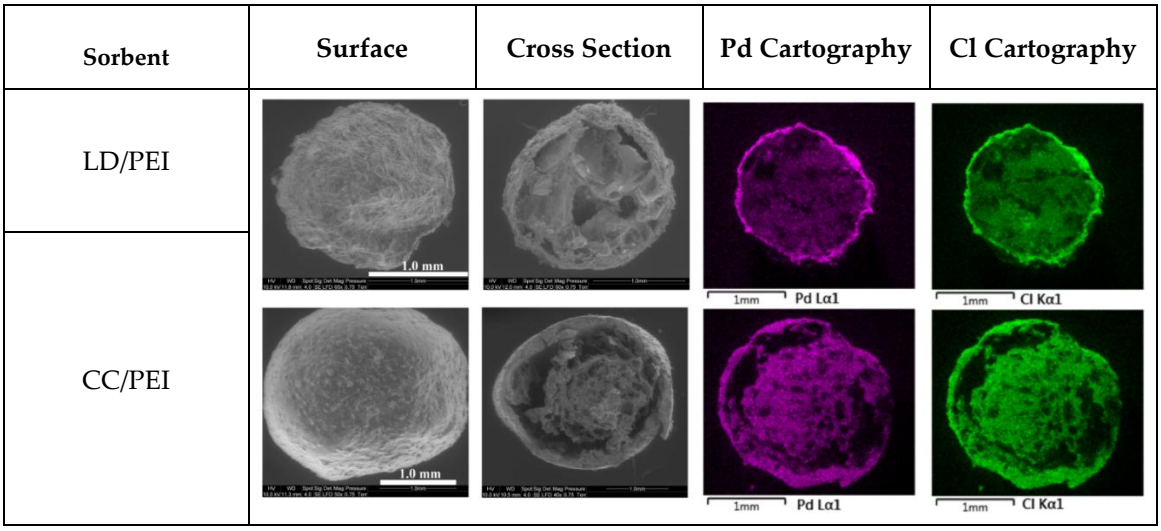

Figure 2. SEM (Scanning electron microscopy) micrographs of the raw beads and element cartographies of Pd-loaded beads.

The FTIR spectrophotometric analysis of raw sorbents, blank beads, and Pd-loaded beads was performed to identify the functional groups of the materials and to understand the binding mechanism. The spectra are shown in Supplementary Materials Figure S4, while the assignments of the main bands are reported in Supplementary Materials Table S1. The band observed in the spectrum of *L. digitata* at 3278 cm^{-1} corresponds to O–H vibration [26]. The band at 2935 cm^{-1} is assigned to the C–H stretching [27]. The peaks at 1605, 1416, 1250, and 1022 cm^{-1} represent COO– asymmetric stretching [28], COO– symmetric stretching [29,30], CH_3 symmetric bending [31], and C–O–C anti-symmetric stretching [32,33], respectively. For *C. crispus* biomass, the main bands relate to –OH overlapping (3283 cm^{-1}) [26], C–H stretching (2924 cm^{-1}) [27], C=C stretching (1644 cm^{-1}) [34], N–H bending and C–N stretching (1531 cm^{-1}) [35], COO− symmetric stretching (1416 cm^{-1}) [29,30], S–O stretching (1152 and 1221 cm^{-1}) [36,37], C−O−C antisym. stretching (1152 and 1034 cm^{-1}) [32,33], and CH bending (696 cm^{-1}) [38]. In a word, the main functional groups on *L. digitata* are hydroxyl and carboxyl groups, while for *C. crispus*, besides these two reactive groups, sulfate groups are also identified. Indeed, brown algae (*L. digitata*) contain 31% of alginate which can provide a certain amount of carboxyl groups, while the carrageenan on red algae (*C. crispus*) bears ester sulfate groups. Both carboxyl and ester sulfate groups can be involved in metal binding.

After the incorporation of PEI-GA, the peaks appear at 2856 cm^{-1} and 2854 cm^{-1} for LD/PEI and CC/PEI beads, respectively, and the $(CH_2)_n$ band around 2947 cm^{-1} appears more distinct because of the number of C–H groups present in PEI and GA [39]. The peaks at 1599 cm^{-1} for LD/PEI beads

and 1610 cm^{-1} for CC/PEI beads correspond to C=N vibration, which is due to the reaction between primary amine groups of PEI and GA, forming "Schiff's base" [40]. The peak at 1605 cm^{-1} (COO− asymmetric stretching) on LD beads disappears, which could be attributed to the overlapping with C=N vibration. Other changes on LD beads include band shift from 1416 cm^{-1} to 1397 cm^{-1} (COO− symmetric stretching) and the disappearance of the peak at 1250 cm^{-1} (C−O stretching), confirming the ionic crosslinking reaction between positively charged amino groups of PEI and the negatively charged carboxylate groups on *L. digitata*. At the same time, for CC beads, there are some changes in the wave number for C=C stretching and COO− symmetric stretching. Moreover, a decrease in the intensity of S−O stretching mode (1221 cm^{-1}) of the sulfate ester group is also observed. This is probably because some of the negatively charged sulfate ester reacted with the positively charged amine groups on PEI and this resulted in physicochemical changes of carrageenan. Indeed, a previous study [16] showed that protonated amine groups of PEI interact with sulfate groups of κ-carrageenan (κC), enabling the formation of the PEI-κC polyelectrolyte complex.

After Pd(II) sorption, the main change is the shift of the C=N vibration peak from 1599 cm^{-1} to 1608 cm^{-1} for LD/PEI, and from 1610 cm^{-1} to 1621 cm^{-1} for CC/PEI beads, confirming the contribution to Pd(II) sorption through the incorporation of PEI-GA into the beads. For LD/PEI beads, a new peak began appearing at 1711 cm^{-1}, assigned to the carboxylic acid C=O stretching, while the COO– peak at 1397 cm^{-1} disappeared; this means that a part of the carboxyl groups are converted to the anhydride form, which could be due to the excess of protons in acid solution (sorption was performed at pH 1) [41].

3.2. Pd(II) Sorption in Mono Metal System

3.2.1. pH Effect

The pH effect was studied within the pH range of 0.3–4.0 adjusted by H_2SO_4 or NaOH. The data shown in Figure 3 indicate that Pd(II) binding onto both *L. digitata*-based and *C crispus*-based beads is pH-dependent. The sorption of Pd(II) onto functionalized sorbents can be mainly attributed to: (1) coordination (i.e., via a ligand exchange mechanism on amine, carboxyl groups); and (2) electrostatic attraction between positively charged amine groups and anionic chloro-metal complexes. For the former one, a low pH is not favorable to metal sorption due to the increased competition between protons and Pd(II), while for the latter one, a low pH is usually required to positively charge the amine groups. It is noteworthy that, in this study, the concentration of HCl in the initial solution was around 0.09 M (diluted from stock solution), resulting in the predominance of chloroanionic species: $PdCl_4^{2-}$ (96%), $PdCl_3^-$ (3 ~ 4%), and $PdCl_2$(aq) (0.1%) throughout the pH range. Therefore, Pd(II) binding occurs mainly through electrostatic attraction. Figure S5 shows the pH before and after the sorption process. The pH does not change after sorption for CC/PEI beads. However, for LD/PEI beads, due to a relatively higher pH_{PZC} value of LD/PEI (7.79) than that of CC/PEI beads (6.80), the solution pH increases significantly after sorption when the initial pH is higher than 3. The pK_a values of primary, secondary, and tertiary amine groups on bPEI were reported as 4.5, 6.7, and 11.6, respectively [15]. Thus, in acidic media, the protonation of amino groups leads to the improvement of the sorption of chloro-anionic palladium species through electrostatic attraction. In addition, the encapsulating matrix is made of alginate (i.e., guluronic and mannuronic acid groups with pK_a of 3.65 and 3.38, respectively [42]) for *L. digitata* and κ-carrageenan (i.e., sulfonate groups of carrageenan with pK_a close to 4.9 [43]) for *C. crispus*. Indeed, Sekkal et al. [44] reported that κ-carrageenan is the predominant carrageenan type in *C. crispus*. At a pH below 4, most of these groups are protonated and poorly active for binding palladium chloro-anions. When the pH_{eq} is lower than 4, the maximum binding for both beads is observed at pH 1 with a sorption capacity of 0.88 ± 0.03 mmol g^{-1} for LD/PEI and 1.37 ± 0.02 mmol g^{-1} for CC/PEI beads. Ricoux et al. [45] reported that a decrease of pH (below 4) reduced the amount of palladium sorbed on functionalized macroreticular Amberlite XAD resins with sulfur and nitrogen ligands. In their case, the Pd binding was mainly attributed to a coordination

mechanism; the competition from protons for the active binding sites when decreasing the solution pH would reduce the coordination between Pd(II) and the above ligands. While the pH continues decreasing (a greater amount of acid added), the sorption capacity decreases gradually. This could be due to the competition of a huge amount of SO_4^{2-} in the solution (due to the effect of different anions will be discussed in the next section below). The dramatic increase in Pd(II) binding onto LD/PEI as pH_{eq} increases to 4.7 could be attributed to the metal precipitation effect (the formation of low soluble Pd(II) species). Indeed, Natale et al. [5] reported that the Pd(II) sorption onto activated carbon could be accompanied by microprecipitation phenomena when the pH > 3 (C_0: 50 mg L^{-1}, chloride concentration: 0.1 M, pH controlled by NaOH).

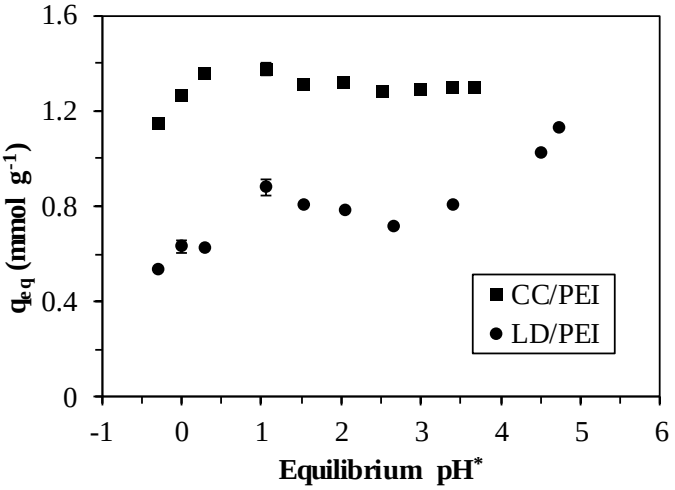

Figure 3. Effect of pH on Pd(II) sorption onto LD/PEI and CC/PEI (C_0: 0.8 $mmol^{-1}$; contact time: 72 h; temperature: 20 °C; SD: 0.25 g L^{-1}; *: the "negative values of pH correspond to HCl concentrations ranging between 0.1 M and 1 M").

3.2.2. Uptake Kinetics

The kinetics of Pd(II) sorption onto LD/PEI and CC/PEI beads at two different stirring speeds are shown in Figure 4a. In a solid-liquid sorption process, adsorbate transfer can be controlled by resistances to film diffusion (so called external diffusion), surface diffusion, and pore diffusion, or combined surface and pore diffusion. A higher agitation speed is supposed to decrease the boundary layer (resistance to film diffusion) and thus increase the speed at which the sorption system reaches equilibrium [46,47]. In this study, the kinetic behaviors obtained from 60 rpm and 150 rpm are almost overlapped, even during the first few hours, suggesting that the external film diffusion should not be the main controlling factor. In general, LD/PEI beads present slightly faster kinetics than CC/PEI beads. The plots of q_t/q_{eq} against t in Supplementary Materials in Figure S6 confirm this phenomenon more clearly: LD/PEI beads reach the equilibrium at 24 h, while more than 48 h are required for CC/PEI beads. As discussed in the SEM-EDX analysis section, the PEI-GA particles are mostly distributed in the outer layer of LD/PEI beads and over the whole mass of CC/PEI beads. Hence, for LD/PEI beads, the reaction rate was mainly controlled by surface diffusion, pore diffusion, and sorption itself, whereas for CC/PEI beads, the internal diffusion proceeded in parallel with the sorption reaction and this is expected to require more time for reaching equilibrium. Another reason could be the smaller size of LD/PEI beads (2.48 ± 0.18 mm) compared to CC/PEI beads (3.33 ± 0.17 mm). Three models including the Pseudo-second order rate equation (PSORE), the Pseudo-first order rate equation (PFORE), and Intraparticle diffusion model equation (IPDE) were used to fit the experimental data. The parameters for the PFORE and PSORE were obtained by non-linear regression analysis and the data before equilibrium time (24 h for LD/PEI and 48 h for CC/PEI beads) were used for modeling. The PSORE fits the experimental data better compared to the PFORE, regardless of the

sorbent. The solid lines in Figure 4a represent the fit of the experimental data with the PSORE and the modeling parameters are reported in Table 1. The predicted equilibrium sorption capacities ($q_{e,cal}$) from PSORE for both beads are in agreement with those obtained from the experiment ($q_{e,exp}$). However, although the PSORE can adequately predict the sorption kinetics, it does not show the sorption mechanisms, while the intraparticle diffusion model helps in identifying the reaction pathways and sorption mechanisms and reveals the rate-controlling step. As shown in Figure 4b, the plot of q_t against $t^{0.5}$ presents multiple linear regions, indicating that the sorption process is controlled by a multistep mechanism [47]. Two main stages before achieving equilibrium can be identified in the plots of Pd(II) sorption onto both LD/PEI and CC/PEI sorbents. The first step represents the mass transfer controlled by the resistance to surface diffusion. During this step, a large amount of Pd(II) is bound to the sorption sites that are readily accessible. The second stage refers to the step controlled by the resistance to intraparticle diffusion including pore diffusion and along pore-wall surfaces [22,47]. At this stage, the sorption rate is far slower than that for the first stage ($k_{id,2}$<<$k_{id,1}$, shown in Table 1). The same trend was observed in previous studies, for the sorption of dye onto ZnO nanoparticles [48] and Pb(II) binding on the Cu/ZnO composite [49]. The values of intercept C are non-zero, suggesting that the sorption process is not only controlled by intraparticle diffusion: the resistance to film diffusion plays a role in the overall uptake kinetics.

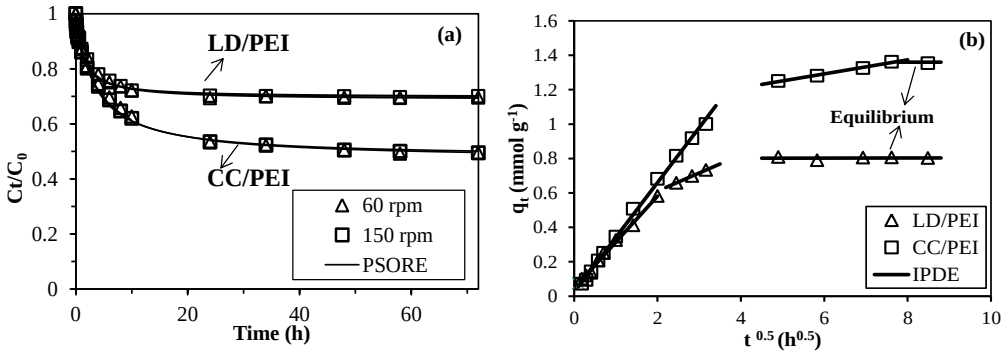

Figure 4. Uptake kinetics for Pd(II) sorption using LD/PEI and CC/PEI beads: (**a**) Modeling with PSORE (pseudo-second order rate equation); (**b**) Modeling with IPDE (intraparticle diffusion equation) at an agitation speed of 60 rpm (C_0: 0.5 mmol L^{-1}; SD: 0.2 g L^{-1}; pH: 1, adjusted by H_2SO_4 or NaOH; room temperature).

Table 1. Uptake kinetics—Modeling parameters for PFORE, PSORE, and IPDE (agitation speed: 60 rpm). LD/PEI: *L. digitata*-bPEI-GA composite; CC/PEI: *C. crispus*-bPEI-GA composite; PFORE: pseudo-first order rate equation; PSORE: pseudo-second order rate equation; IPDE: intraparticle diffusion equation.

Model	Parameter	LD/PEI	CC/PEI
Experiment	$q_{eq,exp}$ (mmol g^{-1})	0.81	1.36
PFORE	$q_{eq,calc}$ (mmol g^{-1})	0.77 (0.041)	1.30 (0.038)
	$k_1 \times 10^3$ (min^{-1})	7.51 (1.07)	3.03 (0.32)
	R^2	0.94	0.97
PSORE	$q_{eq,calc}$ (mmol g^{-1})	0.82 (0.037)	1.42 (0.032)
	$k_2 \times 10^3$ (g $mmol^{-1}$ min^{-1})	14.42 (2.13)	3.08 (0.42)
	R^2	0.97	0.99
IPDE	$k_{id,1}$ (mmol g^{-1} $h^{-0.5}$)	0.267 (0.008)	0.319 (0.006)
	C_1	0.047 (0.008)	0.022 (0.01)
	R_1^2	0.99	0.99
	$k_{id,2}$ (mmol g^{-1} $h^{-0.5}$)	0.105 (0.001)	0.041 (0.003)
	C_2	0.400 (0.001)	1.047 (0.02)
	R_2^2	0.99	0.99

into parenthesis: standard error.

3.2.3. Sorption Isotherms

The sorption isotherms were conducted at pH 1 to compare the sorption capacities of LD/PEI beads and CC/PEI beads, as well as the corresponding blank beads (i.e., LD and CC beads, respectively). As mentioned above, due to the amount of hydrochloric acid (1.1 M) in the mother solution, the predominant palladium species in those diluted working solutions is $PdCl_4^{2-}$ (96%). Therefore, the complexation of free Pd(II) onto carboxylate groups in *L. digitata* or sulfate groups in *C. crispus* should be limited. The protein in those algae (8–15% in *L. digitata*, and around 10% in *C. crispus* [50]) should play the main role in Pd(II) sorption; indeed, proteins bear a certain amount of amino-acid moieties that can bind the anion complex through electrostatic attraction. Figure 5 shows that the sorption capacities of the two blank beads are quite low: 0.11 mmol g^{-1} for LD beads and 0.04 mmol g^{-1} for CC beads, while those of LD/PEI and CC/PEI beads are significantly improved due to the loading of PEI-GA. Moreover, CC/PEI beads show a much higher sorption capacity when compared to LD/PEI beads. Although the same amount of PEI was used for modifying both beads during the synthesis procedure, as mentioned above, the repulsive force of the outer Ca(II)-alginate barrier decreases the amount of PEI penetrating into the core of LD/PEI beads and thus results in a lower metal binding. To have a better understanding of the sorption mechanism and the relationship between the amount of adsorbate adsorbed on the sorbents and the concentration of adsorbate in the liquid at the equilibrium, several models (i.e., Langmuir, Freundlich, and Sips models) were applied to simulate the experimental data. While the Langmuir isotherm describes monolayer adsorption, the Freundlich equation assumes non-ideal and reversible adsorption (not restricted to the formation of a monolayer). As a combined form of these two models, the Sips isotherm predicts the heterogeneous sorption systems and circumvents the limitation of the rising adsorbate concentration associated with the Freundlich isotherm model; at low metal concentrations, it reduces to the Freundlich isotherm, while at high concentrations, it represents the monolayer sorption characteristic of the Langmuir isotherm [51]. The determination coefficients (R^2, shown in Table 2) show that the Sips equation with a greater number of parameters can describe all the experimental isotherms well, but it overestimates the maximum sorption capacity for CC and CC/PEI beads. Conversely, although the Langmuir model presents a slightly lower R^2 for CC-based beads, it predicts more precisely maximum sorption capacities.

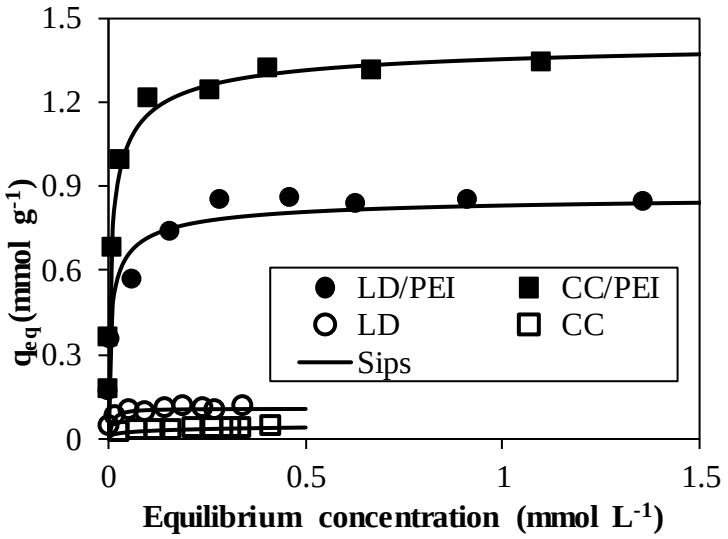

Figure 5. Pd(II) sorption isotherms using raw algal biomass, LD/PEI, and CC/PEI beads (SD: 0.5 g L^{-1}; pH: 1, adjusted by H_2SO_4 or NaOH; Contact time: 72 h; T: 20 °C). Note: CC beads were degraded after the sorption process.

Table 2. Sorption isotherms—Modeling parameters for the Langmuir, Freundlich, and Sips equations.

Model	Parameter	LD	CC	LD/PEI	CC/PEI
	$q_{eq,exp}$ (mmol Pd g^{-1})	0.11	0.04	0.85	1.34
Langmuir	$q_{eq,cal}$ (mmol Pd g^{-1})	0.11 (0.01)	0.04 (0.00)	0.81 (0.03)	1.31 (0.05)
	b (L $mmol^{-1}$)	112.67 (30.47)	26.79 (7.69)	262.71 (102.8)	129.01 (32.3)
	R^2	0.95	0.91	0.88	0.96
Freundlich	K_F (mmol g^{-1})/(mmol L^{-1})^n	0.14 (0.03)	0.05 (0.01)	0.90 (0.04)	1.47 (0.09)
	n	0.16 (0.04)	0.24 (0.03)	0.16 (0.03)	0.16 (0.03)
	R^2	0.77	0.97	0.90	0.89
Sips	$q_{eq,cal}$ (mmol Pd g^{-1})	0.11 (0.01)	0.08 (0.01)	0.88 (0.08)	1.44 (0.05)
	b (L $mmol^{-1}$)	382.54 (93.44)	1.18 (0.43)	16.64 (5.72)	15.66 (5.69)
	n	0.80 (0.02)	2.66 (1.07)	1.72 (0.07)	1.71 (0.06)
	R^2	0.96	0.96	0.95	0.99

into parenthesis: standard error.

In Supplementary Materials, Table S2 compares the Pd(II) sorption capacity of a variety of sorbents. Both LD/PEI and CC/PEI beads show a much higher sorption capacity than unmodified biosorbents such as *R. lanuginosum* biomass [52], raw alginate beads, and algal beads [53], and comparable sorption levels compared to chemically modified alginate beads [54]. While modified XAD-7 resins [55–57] shown in the table present lower sorption capacities than CC/PEI beads, *p*-Sulfonatothiacalix [6] arene-impregnated IRA-411 or IRA-400 resins [57] show a much higher sorption capacity. However, the beads are environmentally friendly and low-cost; these properties also make them attractive for practical application.

3.3. Pd(II) Sorption in Complex Systems

3.3.1. Effect of Anions and Cations

The effect of anions was studied by adding different concentrations of NaCl, $NaNO_3$, or Na_2SO_4 into initial solution containing a Pd(II) concentration of 0.8 mmol L^{-1} and chloride concentration of 0.09 M (diluted from mother solution). Figure 6 shows that with the increasing concentration of the salts, the sorption capacity decreases, regardless of the sorbent. The addition of NO_3^- and Cl^- may influence Pd(II) sorption through different mechanisms [45], depending on the main functional groups on the sorbents and the speciation of Pd(II):

(1) If Pd(II) sorption occurs through metal-ligand coordination, such as Pd(II) bound onto carboxyl group-based alginate beads [53], chloride or nitrate anions in the solution may compete with the ligands on the sorbents for coordinating Pd(II). Thus, increasing such anions will reduce the amount of palladium bound to the sorbents, such as Pd(II) sorption onto calcium alginate beads reported by Cataldo et al. [58];

(2) If Pd(II) sorption occurs via electrostatic attraction between positively charged amine groups and negatively charged anionic palladium complexes, at the beginning, the addition of NaCl or $NaNO_3$ can promote the formation of $PdCl_3^-$, $PdCl_4^{2-}$, or $Pd(NO_3)_3^-$, and consequentially increase the sorption capacity. However, when the concentration of these anions increases, anions may compete with chloro-anionic palladium species for binding on amine groups and the sorption capacity decreases. For example, Nagireddi et al. [59] reported an increase of palladium sorption onto chitosan (amine group-based sorbent) when the concentration of chloride increased from 0 to 33 mg L^{-1}, followed by a significant decrease of metal binding when the chloride concentration continued growing up to 500 mg L^{-1}. Similarly, Sharma et al. [60] observed that a maximum Pd(II) sorption capacity could be achieved for amine-functionalized resin when the concentration of chloride was 0.1 M;

(3) If the bond between Pd(II) and the sorbents is not ionic, Pd(II) sorption could be almost independent on salinity variation, such as Pd(II) sorption onto activated carbon [5].

It is noted that, in this study, due to the high chloride concentration diluted from the mother solution, the predominant palladium species in the experiments are $PdCl_4^{2-}$ and $PdCl_3^-$. Therefore, Cl^-, NO_3^-, and SO_4^{2-} will compete with the chloro-palladium complexes for the binding sites; the sorption capacity decreases gradually when the concentration of these salts increases. Interestingly, the effect of SO_4^{2-} on Pd(II) binding is slightly less marked compared to the other two anions. Similarly, Su et al. [61] studied the effect of a series of anions on As removal and concluded that sulfate anions have a lower impact on As removal compared to other anions such as nitrate. It is probably due to the lower affinity of the functional groups (i.e., amine groups in this study) for sulfate than for other anions.

The influence of different cations on Pd(II) sorption was investigated by adding $Fe_2(SO_4)_3$, $CuSO_4$, and $Al_2(SO_4)_3$ salt to palladium solution. The results in Figure 7 show that the trends of those salts are similar but Cu(II) exhibits a slightly higher inhibition on Pd(II) sorption. As discussed above, Pd(II) sorption occurs mainly through electrostatic attraction. Thus, the influence of metal cations should be limited. However, those cations may influence the sorption by forming metal sulfate complexes. The free sulfate anions in the solution are thus reduced and this leads to less competition between these anions and $PdCl_3^-$ or $PdCl_4^{2-}$ for the sorption sites. Indeed, as shown in Supplementary Materials Table S3, the addition of the salts does not significantly change palladium speciation in the solution. While a certain amount of SO_4^{2-} are captured by Fe^{3+} and Al^{3+} to form $FeSO_4^+$ and $AlSO_4^+$, respectively, most of the SO_4^{2-} in the solution added with $CuSO_4$ exists as SO_4^{2-} (19.6%) and HSO_4^- (74.6%); These anions are likely to compete with chloro-palladium complexes for the sorption sites.

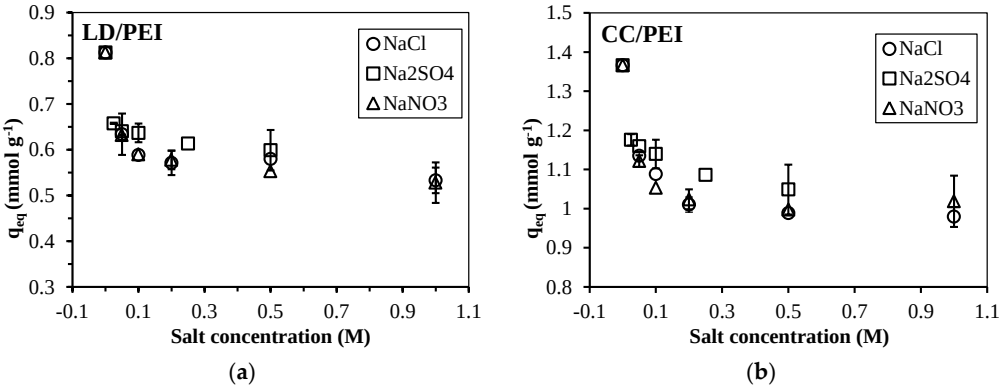

Figure 6. Influence of anions on Pd(II) sorption using (**a**) LD/PEI and (**b**) CC/PEI beads (C_0: 0.8 mmol L^{-1}; SD: 0.25 g L^{-1}; pH: 1, adjusted by H_2SO_4 or NaOH; Contact time: 72 h; T: 20 °C).

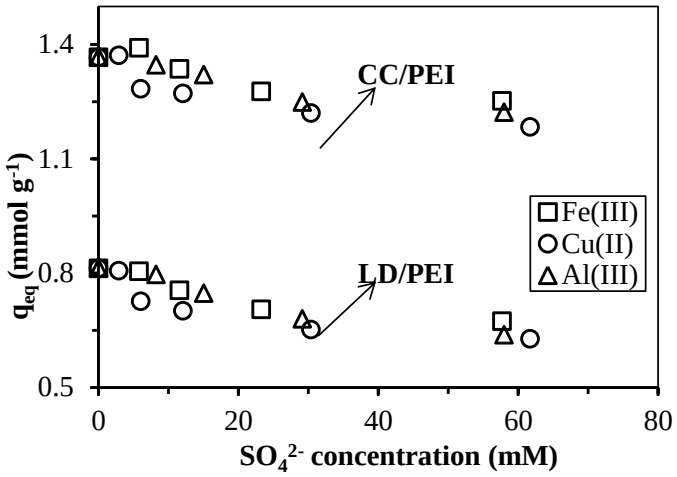

Figure 7. Influence of metal ions on Pd(II) sorption using LD/PEI and CC/PEI beads (C_0: 0.8 mmol L^{-1}; SD: 0.25 g L^{-1}; pH: 1, adjusted by H_2SO_4 or NaOH; Contact time: 72 h; T: 20 °C).

The influence of platinum on palladium sorption has been carried out at pH 1 with different concentrations of platinum, while the concentration of palladium was fixed at 0.5 mmol L^{-1}. The results in Figure 8 show that with the increase of Pt(IV) concentration from 0 to 0.5 mmol L^{-1}, the sorption capacity of LD/PEI for Pd(II) decreases from 0.80 to 0.57 mmol g^{-1}, while in the case of CC/PEI, it decreases from 1.35 to 1.09 mmol g^{-1}. However, the sorption capacity for Pt(IV) rises from 0 to 0.22 mmol g^{-1} for LD/PEI and to 0.35 mmol g^{-1} for CC/PEI beads. The molar ratio of Pd(II) to Pt(IV) loaded on LD/PEI and CC/PEI beads is 2.59 and 3.11, respectively, when the initial solution contains an equal amount (0.5 mmol L^{-1}) of Pd(II) and Pt(IV). Therefore, although the presence of Pt(IV) affected the sorption of Pd(II), the sorbents maintain a preference for Pd(II) over Pt(IV).

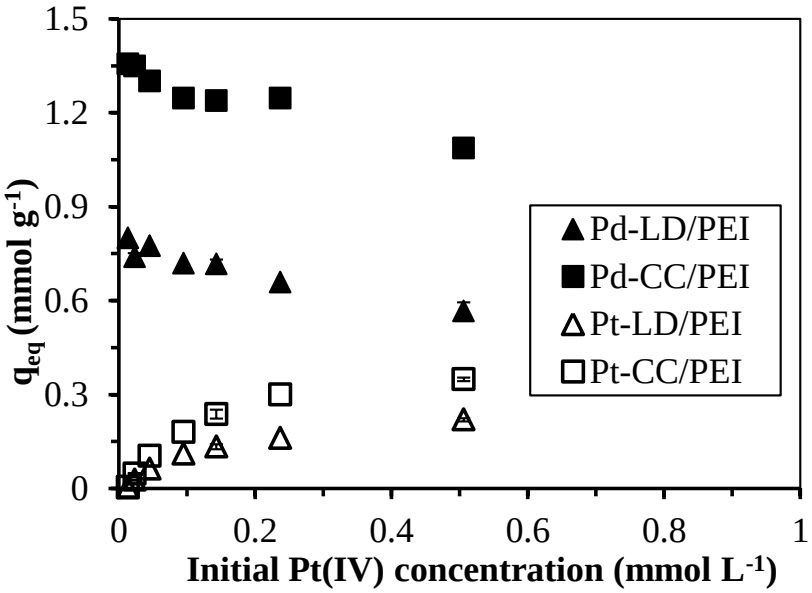

Figure 8. Influence of different concentrations of Pt(IV) on Pd(II) sorption using LD/PEI and CC/PEI beads (C_0: 0.8 mmol L^{-1}; SD: 0.25 g L^{-1}; pH: 1, adjusted by H_2SO_4 or NaOH; Contact time: 72 h; T: 20 °C).

3.3.2. Application to the Treatment of "Synthesized" Wastewaters

To evaluate the application potential of the beads for recovering Pd(II) from industrial effluents, the sorbents were applied to two different synthesized leaching liquors from a spent catalyst and a car catalytic converter, respectively.

Figure 9 shows the results of Pd(II) recovery from the spent catalyst leachate. Due to the presence of a high concentration of chloride ions, the sorption capacities of the beads are much less than those in a single-metal system. The sorption efficiencies of LD/PEI and CC/PEI beads are 81.2% and 97.4%, respectively, with a sorbent dose of 1 g L^{-1}. Using acidic thiourea as the desorption agent, more than 90% of the loaded Pd(II) was desorbed, contributing to a Pd(II) recovery percentage of 75% and 88% for LD/PEI and CC/PEI beads, respectively. The concentration factor (CF) was calculated as the ratio of the Pd(II) concentration in desorption agent to the initial concentration in synthesized leachate. The concentration factor is 3.76 for LD/PEI and 4.39 for CC/PEI. The photo on the right shows the sorbents after the sorption process. The sorbents are stable in the background electrolyte (2 M NaCl, 0.5 M HCl): the beads are not damaged after sorption and desorption processes.

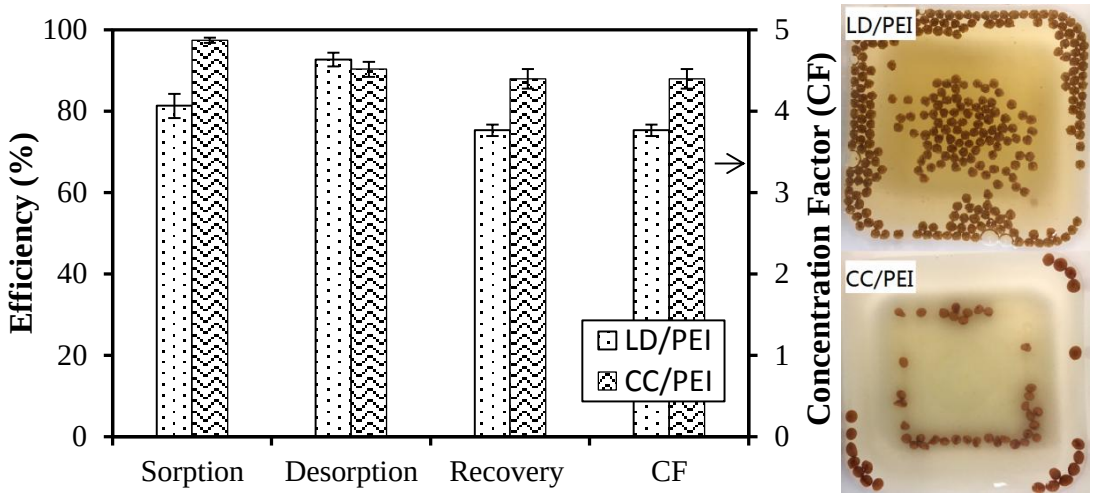

Figure 9. Pd(II) recovery from synthesized leachate of spent catalysts (Sorption step: V: 100 mL; mass: 100 mg (dry weight); time: 72 h; temperature: 20 °C—desorption step: 0.1 M HCl/0.2 M Thiourea solution; V: 20 mL; time: 24 h; temperature: 50 °C). CF: concentration factor.

The results of Pd(II) recovery from the leachate of the car catalyst converter are presented in Figure 10. The initial solution contains 0.38 mmol L^{-1} of Pd(II), 0.07 mmol L^{-1} of Pt(IV), 2.93 mmol L^{-1} of Fe(III), 91.03 mmol L^{-1} of Al(III), 2.47 mmol L^{-1} of Ce(III), and 0.61 mmol L^{-1} of Zn(II), while in the desorption solution, the concentration of Pd(II) and Pt(IV) increases to 1.37 and 0.17 mmol L^{-1}, respectively, for LD/PEI and 1.70 and 0.20 mmol L^{-1}, respectively, for CC/PEI beads. The concentration of other base metals is negligible, except for Al(III), which is close to 0.5 mmol L^{-1} for both LD/PEI and CC/PEI beads. The recovery efficiency is close to 72% and 89% for LD/PEI and CC/PEI beads, respectively, with a sorbent dosage of 0.5 g L^{-1}. The enrichment factor (EF, calculated as the molar percentage of metal in the initial solution divided by its molar percentage in the desorption solution) of Pd(II) is 167.7 for LD/PEI and 177.5 for CC/PEI.

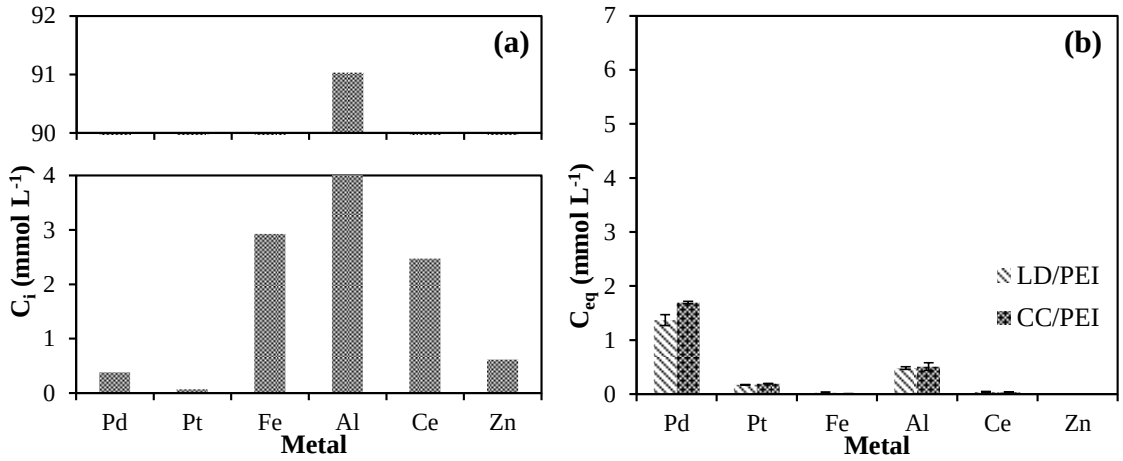

Figure 10. Treatment of the synthesized leaching liquor of the autocatalytic converter using LD/PEI and CC/PEI beads: (**a**) composition of the initial leachate; and (**b**) composition of the eluate after the sorption-desorption process (Sorption step: V: 100 mL; mass: 50 mg (dry weight); time: 72 h; temperature: 20 °C—desorption step: 0.1 M HCl/0.2 M Thiourea solution; V: 20 mL; time: 24 h; temperature: 50 °C).

4. Perspectives

The feasibility of applying these two kinds of beads for the recovery of Pd(II) from acid liquors (HCl or H_2SO_4) with a large amount of NaCl or base metals has been confirmed. The repulsive force of the outer Ca(II)-alginate barrier of LD beads makes it difficult for PEI to penetrate through the layer and get access to the inner compartment, resulting in a lower recovery efficiency of LD/PEI compared to CC/PEI beads. Therefore, CC/PEI beads seem to be more promising for practical applications related to the recovery of Pd(II) from the leaching liquors. However, their high stability allows their implementation not only as sorbents for Pd(II) recovery, but also as catalysts after the reduction of loaded Pd(II). It was reported that when applied as supported catalysts, even loaded with a small amount of Pd such as 5% (*w*/*w*) [62], the catalyst can be effective. This means that the sorption capacity of LD/PEI for Pd(II) is enough to be applied as supported catalysts. Therefore, future studies will focus on the test of these materials for catalytic hydrogenation. The effect of metal distribution will be compared: the outer layer for the LD/PEI-Pd catalyst versus uniform dispersion for the CC/PEI-Pd catalyst.

5. Conclusions

Two kinds of beads, alginate-based and carrageenan-based algal beads (LD and CC beads, respectively) gelled by Ca-alginate and K-carrageenan, respectively, and then modified with polyethyleneimine (PEI) and glutaraldehyde (GA) by using the impregnation method, were compared for Pd(II) recovery. Results show that due to the Ca-alginate barrier, functional material-PEI can hardly get access to the sites in the core of LD beads: a lower amount of PEI is incorporated in LD/PEI beads compared to CC/PEI beads, where the PEI diffusion barrier is negligible. This phenomenon leads to a lower sorption efficiency but faster sorption kinetics of LD/PEI compared to the CC/PEI composite. Moreover, when applied to treat synthesized leaching liquors from a spent catalyst and a waste car catalytic converter, the two sorbents are stable, but CC/PEI beads have a higher Pd recovery efficiency.

Supplementary Materials: The following are available online at www.mdpi.com/2076-3417/8/2/64/s1, Figure S1: The preparation process of LD/PEI and CC/PEI beads, Figure S2: The sorption capacity of the beads prepared at two different times (Dose: 0.5 g L^{-1}; pH: 1-adjusted by H_2SO_4 or NaOH; Contact time: 72 h; T: 20 °C), Figure S3: EDX analysis of LD/PEI and CC/PEI beads before and after Pd(II) sorption, Figure S4: FTIR spectra of the raw biomass (*L. digitata* and *C. crispus*), beads (LD/PEI and CC/PEI) and the beads after loading with Pd(II), Figure S5: pH change after sorption process, Figure S6: Plots of q_t/q_{eq} as a function of the time for Pd(II) sorption onto LD/PEI and CC/PEI beads, Table S1: Experimental frequencies of the bands observed for the raw biomass (*L. digitata* and *C. crispus*), beads (LD/PEI and CC/PEI) and the beads after loading with Pd(II). Unit: cm^{-1}, Table S2: Pd(II) sorption properties of a series of sorbents, Table S3: Palladium and anion species when 15 mM SO_4^{2-} (i.e., 5 mM $Fe_2(SO_4)_3$, 15 mM $CuSO_4$, or 5 mM $Al_2(SO4)_3$) were added.

Acknowledgments: S. Wang acknowledges the China Scholarship Council (CSC, Grant N° 20156660002) for providing a PhD fellowship. T. Vincent and E. Guibal acknowledge the European Union's Seventh Framework Programme (FP7/2007-2013) since these results are indirectly derived from a research project (BIOMETAL-DEMO) funded by the FP7 Programme managed by REA-Research Executive Agency (http://ec.europa.eu/research/rea) under Grant N° 699101. Authors thank Jean-Claude Roux (IMT Mines Ales, C2MA) for his technical support for SEM and SEM-EDX analyses.

Author Contributions: Eric Guibal, Thierry Vincent and Shengye Wang conceived and designed the experiments; Shengye Wang and Thierry Vincent performed the experiments; Eric Guibal and Shengye Wang acquired and analyzed the data; Shengye Wang drafted the manuscript; Eric Guibal and Catherine Faur helped perform the analysis with constructive discussions and revised the manuscript.

Conflicts of Interest: The authors declare no conflict of interest.

References

1. Lim, A.; Song, M.-H.; Cho, C.-W.; Yun, Y.-S. Development of Surface-Modified Polyacrylonitrile Fibers and Their Selective Sorption Behavior of Precious Metals. *Appl. Sci.* **2016**, *6*, 378. [CrossRef]
2. Hirano, Y.; Kasai, Y.; Sagata, K.; Kita, Y. Unique approach for transforming glucose to C3 platform chemicals using metallic iron and a Pd/C catalyst in water. *Bull. Chem. Soc. Jpn.* **2016**, *89*, 1026–1033. [CrossRef]

3. Zhou, C.; Ontiveros-Valencia, A.; Wang, Z.; Maldonado, J.; Zhao, H.-P.; Krajmalnik-Brown, R.; Rittmann, B.E. Palladium recovery in a H_2-based membrane biofilm reactor: Formation of Pd (0) nanoparticles through enzymatic and autocatalytic reductions. *Environ. Sci. Technol.* **2016**, *50*, 2546–2555. [CrossRef] [PubMed]
4. Shams, K.; Beiggy, M.; Shirazi, A.G. Platinum recovery from a spent industrial dehydrogenation catalyst using cyanide leaching followed by ion exchange. *Appl. Catal. A Gen.* **2004**, *258*, 227–234. [CrossRef]
5. Di Natale, F.; Orefice, M.; La Motta, F.; Erto, A.; Lancia, A. Unveiling the potentialities of activated carbon in recovering palladium from model leaching solutions. *Sep. Purif. Technol.* **2017**, *174*, 183–193. [CrossRef]
6. Butewicz, A.; Gavilan, K.C.; Pestov, A.; Yatluk, Y.; Trochimczuk, A.; Guibal, E. Palladium and platinum sorption on a thiocarbamoyl-derivative of chitosan. *J. Appl. Polym. Sci.* **2010**, *116*, 3318–3330. [CrossRef]
7. Morisada, S.; Kim, Y.-H.; Ogata, T.; Marutani, Y.; Nakano, Y. Improved adsorption behaviors of amine-modified tannin gel for palladium and platinum ions in acidic chloride solutions. *Ind. Eng. Chem. Res.* **2011**, *50*, 1875–1880. [CrossRef]
8. Guibal, E.; Sweeney, N.V.O.; Zikan, M.; Vincent, T.; Tobin, J. Competitive sorption of platinum and palladium on chitosan derivatives. *Int. J. Biol. Macromol.* **2001**, *28*, 401–408. [CrossRef]
9. Won, S.W.; Kwak, I.S.; Yun, Y.-S. The role of biomass in polyethylenimine-coated chitosan/bacterial biomass composite biosorbent fiber for removal of Ru from acetic acid waste solution. *Bioresour. Technol.* **2014**, *160*, 93–97. [CrossRef] [PubMed]
10. Mahdavinia, G.R.; Bazmizeynabad, F.; Seyyedi, B. *kappa*-Carrageenan beads as new adsorbent to remove crystal violet dye from water: Adsorption kinetics and isotherm. *Desalin. Water Treat.* **2015**, *53*, 2529–2539. [CrossRef]
11. Mahdavinia, G.R.; Iravani, S.; Zoroufi, S.; Hosseinzadeh, H. Magnetic and K^+-cross-linked *kappa*-carrageenan nanocomposite beads and adsorption of crystal violet. *Iran. Polym. J.* **2014**, *23*, 335–344. [CrossRef]
12. Bertagnolli, C.; Grishin, A.; Vincent, T.; Guibal, E. Boron removal by a composite sorbent: Polyethylenimine/tannic acid derivative immobilized in alginate hydrogel beads. *J. Environ. Sci. Health Part A* **2017**, *52*, 359–367. [CrossRef] [PubMed]
13. Wang, S.; Vincent, T.; Roux, J.-C.; Faur, C.; Guibal, E. Innovative conditioning of algal-based sorbents: Macro-porous discs for palladium sorption. *Chem. Eng. J.* **2017**, *325*, 521–532. [CrossRef]
14. Mahdavinia, G.R.; Massoudi, A.; Baghban, A.; Shokri, E. Study of adsorption of cationic dye on magnetic kappa-carrageenan/PVA nanocomposite hydrogels. *J. Environ. Chem. Eng.* **2014**, *2*, 1578–1587. [CrossRef]
15. Willner, I.; Eichen, Y.; Frank, A.J.; Fox, M.A. Photoinduced electron-transfer processes using organized redox-functionalized bipyridinium-polyethylenimine-titania colloids and particulate assemblies. *J. Phys. Chem.* **1993**, *97*, 7264–7271. [CrossRef]
16. Elnashar, M.M.; Yassin, M.A.; Kahil, T. Novel thermally and mechanically stable hydrogel for enzyme immobilization of penicillin G acylase via covalent technique. *J. Appl. Polym. Sci.* **2008**, *109*, 4105–4111. [CrossRef]
17. Zaak, H.; Fernandez-Lopez, L.; Otero, C.; Sassi, M.; Fernandez-Lafuente, R. Improved stability of immobilized lipases via modification with polyethylenimine and glutaraldehyde. *Enzyme Microb. Technol.* **2017**, *106*, 67–74. [CrossRef] [PubMed]
18. Kononova, O.; Kholmogorov, A.; Mikhlina, E. Palladium sorption on vinylpyridine ion exchangers from chloride solutions obtained from spent catalysts. *Hydrometallurgy* **1998**, *48*, 65–72. [CrossRef]
19. Ricoux, Q.; Méricq, J.; Bouyer, D.; Bocokić, V.; Hernandez-Juarez, L.; van Zutphen, S.; Faur, C. A selective dynamic sorption-filtration process for separation of Pd (II) ions using an aminophosphine oxide polymer. *Sep. Purif. Technol.* **2017**, *174*, 159–165. [CrossRef]
20. Lagergren, S. About the theory of so-called adsorption of soluble substances. *Kungliga Sven. Vetenskapsakad.* **1898**, *24*, 1–39.
21. Ho, Y.S.; McKay, G. Pseudo-second order model for sorption processes. *Process. Biochem.* **1999**, *34*, 451–465. [CrossRef]
22. Weber, W.J.; Morris, J.C. Kinetics of adsorption on carbon from solution. *J. Sanit. Eng. Div.* **1963**, *89*, 31–60.
23. Langmuir, I. The adsorption of gases on plane surfaces of glass, mica and platinum. *J. Am. Chem. Soc.* **1918**, *40*, 1361–1403. [CrossRef]
24. Freundlich, H. Over the adsorption in solution. *J. Phys. Chem.* **1906**, *57*, 1100–1107.
25. Sips, R. Combined form of Langmuir and Freundlich equations. *J. Chem. Phys.* **1948**, *16*, 490–495. [CrossRef]

26. Schiewer, S.; Balaria, A. Biosorption of Pb^{2+} by original and protonated citrus peels: Equilibrium, kinetics, and mechanism. *Chem. Eng. J.* **2009**, *146*, 211–219. [CrossRef]
27. Naebe, M.; Wang, J.; Amini, A.; Khayyam, H.; Hameed, N.; Li, L.H.; Chen, Y.; Fox, B. Mechanical property and structure of covalent functionalised graphene/epoxy nanocomposites. *Sci. Rep.* **2014**, *4*, 4375. [CrossRef] [PubMed]
28. Luo, J.; Wang, L.; Mott, D.; Njoki, P.N.; Kariuki, N.; Zhong, C.-J.; He, T. Ternary alloy nanoparticles with controllable sizes and composition and electrocatalytic activity. *J. Mater. Chem.* **2006**, *16*, 1665–1673. [CrossRef]
29. Hofmann, M.P.; Young, A.M.; Gbureck, U.; Nazhat, S.N.; Barralet, J.E. FTIR-monitoring of a fast setting brushite bone cement: Effect of intermediate phases. *J. Mater. Chem.* **2006**, *16*, 3199–3206. [CrossRef]
30. Theras, J.E.M.; Kalaivani, D.; Jayaraman, D.; Joseph, V. Growth and spectroscopic, thermodynamic and nonlinear optical studies of L-threonine phthalate crystal. *J. Cryst. Growth* **2015**, *427*, 29–35. [CrossRef]
31. Wang, L.; Ji, Q.; Glass, T.; Ward, T.; McGrath, J.; Muggli, M.; Burns, G.; Sorathia, U. Synthesis and characterization of organosiloxane modified segmented polyether polyurethanes. *Polymer* **2000**, *41*, 5083–5093. [CrossRef]
32. Wang, X.; Li, D.; Wang, W.; Feng, Q.; Cui, F.; Xu, Y.; Song, X.; van der Werf, M. Crosslinked collagen/chitosan matrix for artificial livers. *Biomaterials* **2003**, *24*, 3213–3220. [CrossRef]
33. Lawrie, G.; Keen, I.; Drew, B.; Chandler-Temple, A.; Rintoul, L.; Fredericks, P.; Grøndahl, L. Interactions between alginate and chitosan biopolymers characterized using FTIR and XPS. *Biomacromolecules* **2007**, *8*, 2533–2541. [CrossRef] [PubMed]
34. Zawadzki, J.; Kaczmarek, H. Thermal treatment of chitosan in various conditions. *Carbohyd. Polym.* **2010**, *80*, 394–400. [CrossRef]
35. Rosu, D.; Rosu, L.; Cascaval, C.N. IR-change and yellowing of polyurethane as a result of UV irradiation. *Polym. Degrad. Stabil.* **2009**, *94*, 591–596. [CrossRef]
36. Tarulli, S.; Quinzani, O.; Piro, O.E.; Castellano, E.E.; Baran, E. Structural and spectroscopic characterization of bis(thiosaccharinato) bis(benzimidazole) cadmium (II). *J. Mol. Struct.* **2006**, *797*, 56–60. [CrossRef]
37. Qiao, J.; Hamaya, T.; Okada, T. New highly proton-conducting membrane poly(vinylpyrrolidone)(PVP) modified poly(vinyl alcohol)/2-acrylamido-2-methyl-1-propanesulfonic acid (PVA–PAMPS) for low temperature direct methanol fuel cells (DMFCs). *Polymer* **2005**, *46*, 10809–10816. [CrossRef]
38. Ríos-Gómez, J.; Lucena, R.; Cárdenas, S. Paper supported polystyrene membranes for thin film microextraction. *Microchem. J.* **2017**, *133*, 90–95. [CrossRef]
39. Lindén, J.B.; Larsson, M.; Kaur, S.; Skinner, W.M.; Miklavcic, S.J.; Nann, T.; Kempson, I.M.; Nydén, M. Polyethyleneimine for copper absorption II: Kinetics, selectivity and efficiency from seawater. *RSC Adv.* **2015**, *5*, 51883–51890. [CrossRef]
40. Tan, I.S.; Lee, K.T. Immobilization of β-glucosidase from *Aspergillus niger* on κ-carrageenan hybrid matrix and its application on the production of reducing sugar from macroalgae cellulosic residue. *Bioresour. Technol.* **2015**, *184*, 386–394. [CrossRef] [PubMed]
41. Xiaohong, G.; Yang, C.Q. FTIR spectroscopy study of the formation of cyclic anhydride intermediates of polycarboxylic acids catalyzed by sodium hypophosphite. *Text. Res. J.* **2000**, *70*, 64–70. [CrossRef]
42. Haug, A. Affinity of some divalent metals to different types of alginates. *Acta Chem. Scand.* **1961**, *15*, 1794. [CrossRef]
43. Sadeghi, M. Synthesis of a biocopolymer carrageenan-g-poly (AAm-co-IA)/montmorilonite superabsorbent hydrogel composite. *Braz. J. Chem. Eng.* **2012**, *29*, 295–305. [CrossRef]
44. Sekkal, M.; Legrand, P.; Huvenne, J.P.; Verdus, M.C. The use of FTIR microspectrometry as a new tool for the identification in situ of polygalactanes in red seaweeds. *J. Mol. Struct.* **1993**, *294*, 227–230. [CrossRef]
45. Ricoux, Q.; Bocokić, V.; Méricq, J.; Bouyer, D.; Zutphen, S.; Faur, C. Selective recovery of palladium using an innovative functional polymer containing phosphine oxide. *Chem. Eng. J.* **2015**, *264*, 772–779. [CrossRef]
46. Choong, T.S.; Chuah, T. Comment on "Separation of vitamin E from palm fatty acid distillate using silica: I. Equilibrium of batch adsorption by BS Chu et al. [Journal of Food Engineering 62 (2004) 97–103]". *J. Food Eng.* **2005**, *67*, 379. [CrossRef]
47. Tran, H.N.; You, S.-J.; Hosseini-Bandegharaei, A.; Chao, H.-P. Mistakes and inconsistencies regarding adsorption of contaminants from aqueous solutions: A critical review. *Water Res.* **2017**, *120*, 88–116. [CrossRef] [PubMed]

48. Zhang, F.; Chen, X.; Wu, F.; Ji, Y. High adsorption capability and selectivity of ZnO nanoparticles for dye removal. *Coll. Surf. A* **2016**, *509*, 474–483. [CrossRef]
49. Modwi, A.; Khezami, L.; Taha, K.; Al-Duaij, O.; Houas, A. Fast and high efficiency adsorption of Pb (II) ions by Cu/ZnO composite. *Mater. Lett.* **2017**, *195*, 41–44. [CrossRef]
50. Fleurence, J. Seaweed proteins: Biochemical, nutritional aspects and potential uses. *Trends Food Sci. Technol.* **1999**, *10*, 25–28. [CrossRef]
51. Foo, K.; Hameed, B. Insights into the modeling of adsorption isotherm systems. *Chem. Eng. J.* **2010**, *156*, 2–10. [CrossRef]
52. Sari, A.; Mendil, D.; Tuzen, M.; Soylak, M. Biosorption of palladium (II) from aqueous solution by moss (*Racomitrium lanuginosum*) biomass: Equilibrium, kinetic and thermodynamic studies. *J. Hazard. Mater.* **2009**, *162*, 874–879. [CrossRef] [PubMed]
53. Wang, S.; Vincent, T.; Roux, J.-C.; Faur, C.; Guibal, E. Pd (II) and Pt (IV) sorption using alginate and algal-based beads. *Chem. Eng. J.* **2017**, *313*, 567–579. [CrossRef]
54. Cataldo, S.; Muratore, N.; Orecchio, S.; Pettignano, A. Enhancement of adsorption ability of calcium alginate gel beads towards Pd (II) ion. A kinetic and equilibrium study on hybrid Laponite and Montmorillonite–alginate gel beads. *Appl. Clay Sci.* **2015**, *118*, 162–170. [CrossRef]
55. Kimuro, T.; Gandhi, M.R.; Kunda, U.M.R.; Hamada, F.; Yamada, M. Palladium (II) sorption of a diethylphosphate-modified thiacalix [6] arene immobilized on amberlite resin. *Hydrometallurgy* **2017**, *171*, 254–261. [CrossRef]
56. Navarro, R.; Saucedo, I.; Gonzalez, C.; Guibal, E. Amberlite XAD-7 impregnated with Cyphos IL-101 (tetraalkylphosphonium ionic liquid) for Pd (II) recovery from HCl solutions. *Chem. Eng. J.* **2012**, *185*, 226–235. [CrossRef]
57. Gandhi, M.R.; Yamada, M.; Kondo, Y.; Shibayama, A.; Hamada, F. *p*-Sulfonatothiacalix [6] arene-impregnated resins for the sorption of platinum group metals and effective separation of palladium from automotive catalyst residue. *J. Ind. Eng. Chem.* **2015**, *30*, 20–28. [CrossRef]
58. Cataldo, S.; Gianguzza, A.; Pettignano, A. Sorption of Pd (II) ion by calcium alginate gel beads at different chloride concentrations and pH. A kinetic and equilibrium study. *Arab. J. Chem.* **2016**, *9*, 656–667. [CrossRef]
59. Nagireddi, S.; Golder, A.K.; Uppaluri, R. Investigation on Pd (II) removal and recovery characteristics of chitosan from electroless plating solutions. *J. Water Process Eng.* **2017**, *19*, 8–17. [CrossRef]
60. Sharma, S.; Rajesh, N. Augmenting the adsorption of palladium from spent catalyst using a thiazole ligand tethered on an amine functionalized polymeric resin. *Chem. Eng. J.* **2016**, *283*, 999–1008. [CrossRef]
61. Su, C.; Puls, R.W. Arsenate and arsenite removal by zerovalent iron: Effects of phosphate, silicate, carbonate, borate, sulfate, chromate, molybdate, and nitrate, relative to chloride. *Environ. Sci. Technol.* **2001**, *35*, 4562–4568. [CrossRef] [PubMed]
62. Choudhary, V.R.; Samanta, C.; Choudhary, T. Factors influencing decomposition of H_2O_2 over supported Pd catalyst in aqueous medium. *J. Mol. Catal. A Chem.* **2006**, *260*, 115–120. [CrossRef]